INVESTIGATION OF THE KINETICS OF CRYSTALLIZATION OF MOLTEN BINARY AND TERNARY OXIDE SYSTEMS

F910373-9

by

JAMES F. BACON, ROBERT B. GRAF, GEORGE K. LAYDEN

JANUARY 1, 1968

United Aircraft Research Laboratories

UNITED AIRCRAFT CORPORATION

EAST HARTFORD, CONNECTICUT

NINTH QUARTERLY PROGRESS REPORT

CONTRACT NASW-1301

United Aircraft Research Laboratories

UNITED AIRCRAFT CORPORATION

EAST HARTFORD, CONNECTICUT

Investigation of the Kinetics of Crystallization of Molten Binary and Ternary Oxide Systems

Quarterly Status Report No. 9

Contract NASW-1301

REPORTED BY J. F. Bacon

R. B. Graf

G. K. Layden

APPROVED BY R. Fanti, Manager
Materials Laboratory

DATE 1/1/68

NO. OF PAGES 35

COPY NO. _____

Investigation of the Kinetics of Crystallization of Molten Binary and Ternary Oxide Systems

Quarterly Status Report No. 9

TABLE OF CONTENTS

Investigation of the Kinetics of Crystallization of Molten Binary and Ternary Oxide Systems

Quarterly Status Report No. 9 - September 1, 1967 through November 30, 1967

Contract No. NASW-1301

SUMMARY

Direct microscopic observation of crystals growing in molten oxides made possible by the micro-furnace previously described has shown that both yttria and more particularly lanthana markedly decrease the rate of crystal growth in the cordierite field. This observation confirms the basic hypothesis of this contract that the likelihood of glass formation in a given system must be regarded as a rate phenomenon as taught by R. W. Douglas.

An important attribute of glass fibers is their strength. Unfortunately glass fibers unless treated chemically to protect them from the atmosphere at the time of their manufacture rapidly deteriorate in strength so that the measurement of this property must be made on virgin glass fibers immediately after preparation. Research to date in this laboratory has concentrated on learning how to attain the correct strength value for readily available commercial glasses such as "E" glass before attempting to characterize the UARL experimental fibers. At this time we are able to measure a strength of 415,000 psi for E glass fibers prepared in our own laboratory in contrast to the published value of 530,000 psi for commercially produced glass fiber. The source of the discrepancy has not yet been resolved but could lie in the fact that the simplified fiber-pulling apparatus employed at UARL may produce fibers whose characteristics are at variance with those produced in the usual commercial fiber bushing.

The number of original glass compositions prepared and melted is now two hundred and eighteen. Glass compositions initiated in the last quarter included nine additional non-silica base glasses but none of these as yet have been successfully made into mechanically-drawn fibers even though readily drawn into fibers by hand. Modulus measurements were carried out on ten additional glass compositions from which glass fibers could be made mechanically at high rates of speed as well as a repetition of one of the UARL higher modulus glasses, number 129. The original twenty samples tested from this glass had an average modulus of 16.5 million psi while twenty samples from a freshly prepared batch of the same glass averaged 16.9 million psi.

In characterizing the glass fibers produced to date more than a thousand modulus measurements have been made. The average deviation to be expected in such measurements has been carefully evaluated. For this reason those glasses which yield occasional high moduli far exceeding the expected range form somewhat of an enigma. In the last tests one glass fiber had a measured modulus of

31.5 million psi, in earlier tests glasses of somewhat similar chemical composition yielded high values of 29.2 million psi and 27.4 million psi. Can such measurements indicate that in some of these fibers a microstructure is present such as a second immiscible glass phase or crystals? Investigations to answer this question have been started at UARL involving transmission electron microscopy of suspect fibers and a deliberate effort to prepare fibers from glasses known to form phase separable systems.

INTRODUCTION

This is the ninth quarterly status report for Contract NASW-1301 entitled "Investigation of the Kinetics of Crystallization of Molten Binary and Ternary Oxide Systems". This ninth quarter starting September 1, 1967 and ending November 30, 1967 formed the second quarter of the second extension to the contract. The primary objective of this contract is to gain a better understanding of the essentials of glass formation by measuring the rate at which crystallization occurs and the effect of anti-nucleating agents on the observed crystallization rate for systems which tend to form complex three dimensional structures. Determination of the crystallization rate may be carried out by continuously monitoring the viscosity and electrical conductivity of the molten system as a function of time and temperature with checks of surface tension at selected temperatures. The crystallization rate may equally well be determined by direct microscopic examination of samples in a micro-furnace as shown in the first section of this report. In this program of research on glass formation the question of whether or not a glass will form is regarded as a rate phenomenon where the probability of such glass formation is greatly increased by employing cooling rates high enough to defeat the formation of the complex many-atom three-dimensional molecule. This view of glass formation justifies the consideration of oxide systems previously thought impractical and allows the search for systems which may yield high strength, high modulus glass fibers to be carried out on an unusually broad basis.

Up to this quarter glasses produced in this program have been largely characterized by studying their fiberization qualities, their density, and their elastic modulus. In general, no effort was made to measure the strength of the glass fibers produced before this quarter, not because we did not think the strength of the glass fibers to be fully as interesting as their elastic moduli, but because the strength is a non-constant characteristic depending on just how soon the measurement is made, the atmosphere present, the method of measurement and other variables. The fiberization characteristics, the elastic moduli of the glass and its density are by contrast, much less ephemeral in nature. The research underway in this laboratory, aimed at measuring a meaningful value for the strengths of the experimental glass fibers produced, forms the second portion of this report.

The third and concluding section of the report is given over to the details of the new glass compositions melted and the physical properties of these compositions excluding strength.

OPTICAL STUDIES OF THE KINETICS OF CRYSTALLIZATION

The measurements of the rate of growth of cordierite in batch 1 were completed, with 30 more data points being taken. All of the data are listed in Table I and are plotted in Fig. 1. The additional data completely delineate the curve depicting the rate of growth of cordierite in batch 1, although the maximum rate of growth and the high temperature end of the curve are the same as in the Summary and Quarterly Status Report No. 7. The maximum growth rate of 485 microns per minute is the fastest we have measured to date. At this rate of growth measurements can be made only for very short times, usually for 30 to 90 seconds. The high temperature end of the curve approaches the liquidus temperature tangentially as discussed in Report No. 7. The scatter in this curve at approximately 1325°C is associated with a change in the morphology of the crystalline aggregate. When the melt is seeded at this temperature, only a few single crystals grow on the thermocouple instead of the rounded masses of crystals which grow at lower temperatures. The measurements of the size of the rounded crystalline aggregates are made by tracing the outlines of the aggregates onto tracing paper and then circumscribing these outlines with a series of concentric circles. It is then easy to measure the change in radius, which represents the change in length of the crystals, as a function of time. Alternately, a circle can be drawn on the polaroid prints and then transferred to a separate piece of paper. This method of measurement cannot be used for the clusters of single crystals, which do not grow with equal velocities. The measurements on these crystals are made along the length of the prism, and the maximum values are reported. All of our measurements are of the change in crystal length as a function of time and do not reflect the amount of glass which has crystallized. This is because of the occurrence of hollow crystals which seem to occur at all temperatures except the higher and lower temperatures; that is, at the faster rates of growth. In batch 1, the three measurements of the rate of solution were made upon aggregates of crystals and are not as accurate as the measurements of the rate of growth. This is because the crystals melt along grain boundaries and drift away from the thermocouple. However, measurement No. 3, at a temperature of 1412 $\pm$ 2°, with a value of -380 microns per minute is sufficiently accurate so that it can be stated that the rate of solution has a very steep negative slope. Solution measurements should be made upon single, solid crystals, which can be grown at temperatures of about 1395° in batch 1.

The rate of growth of cordierite in batch 64 was measured, the data are listed in Table II and plotted in Fig. 2. The composition of this batch, as determined by chemical analysis, is 51.66 wt % SiO_2, 27.92% Al_2O_3, 17.2% MgO, and 3.12% Y_2O_3. The maximum rate of growth of cordierite in this glass is 190 microns per minute, and the liquidus temperature is 1394 $\pm$ 2°. Crystals held at a temperature of 1393 $\pm$ 2° for 20 minutes showed no measureable change in size, and crystals at a temperature of 1395 $\pm$ 2° had a rate of solution of 8 microns per minute. The cordierite which was grown in this glass was nucleated with seed crystals which were suspended in distilled water and then applied to the thermocouple, which was then lowered into the glass in the crucible, just as in the earlier measurements. The cordierite which was grown in this glass had the same crystal habit as that which was observed in batches 1 and 1-B. The X-ray diffraction pattern was also the same as for the cordierite grown in batches 1 and 1-B. Sapphirine was also grown in batch 64 and was apparently nucleated by platinum just as in batch 1.

Table I

Rate of Growth of Cordierite in Batch 1

No.	Temp.	Rate, /min	No.	Temp.	Rate, /min
1	1376 ± 4	0 in. 30 min	23	1032 ± 2	58
2	1189 ± 4	475	24	1400 ± 2	.2
3	1415 ± 3	-20	25	1334 ± 1	100
4	1343 ± 4	11	26	1285 ± 3	275
5	1278 ± 4	250	27	1253 ± 2	485
6	1139 ± 4	360	28	1342 ± 3	80
7	1154 ± 6	320	29	1194 ± 2	450
8	1025 ± 5	42	30	1412 ± 2	-380
9	962 ± 5	5	31	1392 ± 3	0 in. 12 min
10	1278 ± 6	250	32	1316 ± 3	92
11	1297 ± 4	183	33	1407 ± 3	-2
12	1411 ± 5	0 in. 5 min	34	1258 ± 3	475
13	1395 ± 6	0 in. 9 min	35	1086 ± 6	200
14	1355 ± 5	5	36	1128 ± 4	340
15	1220 ± 2	485	37	1101 ± 4	200
16	1155 ± 2	370	38	1322 ± 2	103
17	1428 ± 2	-15	39	1316 ± 3	100
18	1289 ± 2	275	40	1363 ± 3	2.4
19	1282 ± 2	330	41	1296 ± 3	135
20	1011 ± 4	25	42	1305 ± 4	120
21	1061 ± 2	88	43	1328 ± 3	50
22	1249 ± 2	425			

FIG. 1

EFFECT OF TEMPERATURE UPON THE RATE OF GROWTH OF CORDIERITE IN BATCH I

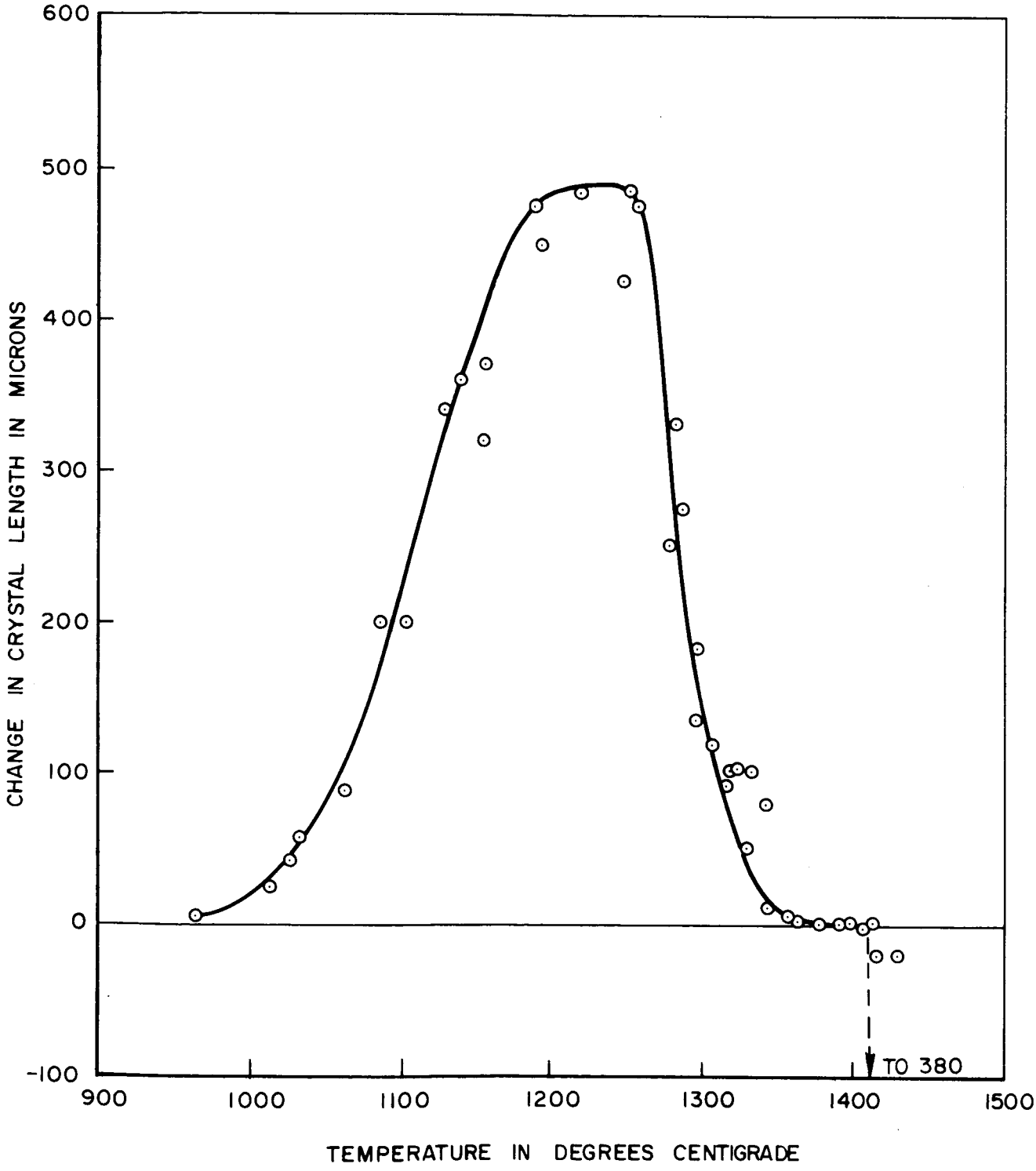

Table II

Rate of Growth of Cordierite in Batch 64

No.	Temp.	Rate	No.	Temp.	Rate
1	1281 ± 2	56	22	1366 ± 4	3
2	1233 ± 2	150	23	1393 ± 2	0 in. 20 min
3	1271 ± 3	75	24	1268 ± 3	120
4	1088 ± 4	88	25	1293 ± 7	58
5	1084 ± 2	80	26	1279 ± 3	100
6	974 ± 6	15	27	1259 ± 6	175
7	1028 ± 4	37	28	1212 ± 2	180
8	1134 ± 2	135	29	1261 ± 4	175
9	1030 ± 6	35	30	1203 ± 2	190
10	1158 ± 4	120	31	1216 ± 6	175
11	1168 ± 4	155	32	1048 ± 2	41
12	1186 ± 4	175	33	1187 ± 2	153
13	1118 ± 4	105	34	1260 ± 4	160
14	1206 ± 2	188	35	1252 ± 3	150
15	1096 ± 3	100	36	1247 ± 2	165
16	1359 ± 8	0 in. 5 min	37	1333 ± 3	8
17	1366 ± 2	2	38	1318 ± 4	18
18	1378 ± 3	0 in. 10 min	39	1143 ± 4	125
19	1395 ± 2	-8	40	1156 ± 2	140
20	1260 ± 4	120	41	1315 ± 2	20
21	1334 ± 4	30	42	1340 ± 2	10

FIG. 2

EFFECT OF TEMPERATURE UPON THE RATE OF GROWTH OF CORDIERITE IN BATCH 64

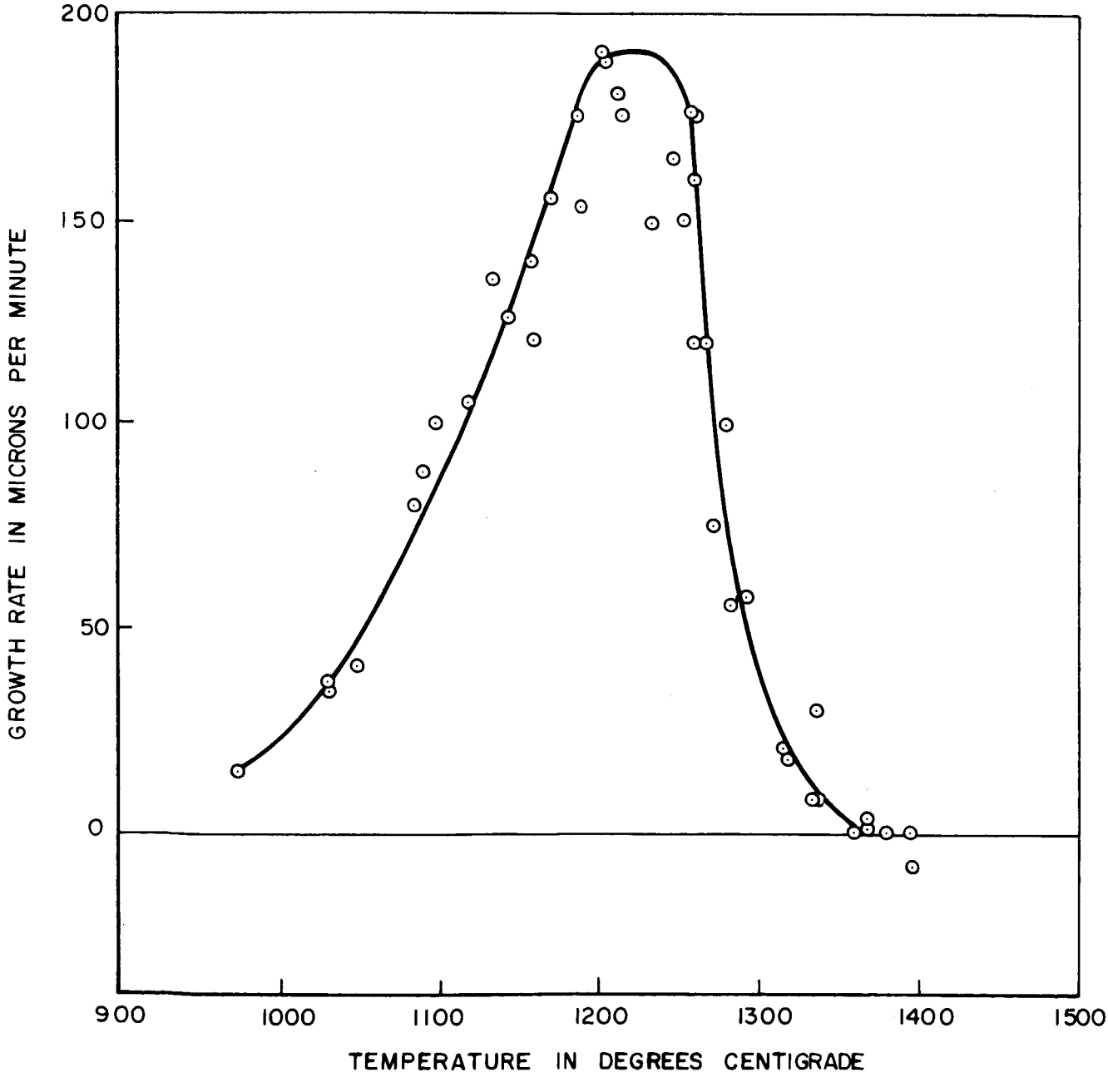

The sapphirine was allowed to crystallize for a longer period of time (3 hours at 1165°) than was that grown in batch 1 and the X-ray diffraction pattern was of better quality, with even better agreement with the data obtained from the ASTM cards.

The rate of growth of cordierite in batch 63 is shown in Fig. 3 and the data are listed in Table III. The composition of this glass, as determined by chemical analysis, is 53.5 wt % SiO_2, 23.08% Al_2O_3, 17.24% MgO, and 5.64% La_2O_3. The maximum rate of growth of cordierite in this glass was 66 microns per minute, which is about 1/3 of the maximum rate observed in batch 64 and about 1/8 of that observed in batch 1. The liquidus temperature of this glass is 1350 $\pm$ 5°. The smaller amount of scatter in this data is due to the slower growth rates, which allow the measurements to be made over longer periods of time, while the measurements of crystal size can be made with the same precision. It is probable that sapphirine will nucleate and grow in this glass as in the others, but this has not yet been determined.

The rate of devitrification of a glass-forming system is usually considered to be proportional to the amount of undercooling below the liquidus temperature and inversely proportional to the viscosity of the system. This suggests that the slower rate of growth in batch 1-B, as compared to that observed in batch 1, is due to increased viscosity because of the higher silica content. In batch 64 (see Table IV for glass compositions, liquidus temperatures, maximum rates of growth and temperatures at which the maximum growth rate occurs), which contains 3.1% yttria in addition to the base glass of magnesia, alumina, and silica, the viscosity versus temperature curve (Fig. 4) is not greatly different from that of batch 1, and yet the maximum rate of growth in No. 64 is less than one-half of that measured in batch 1. In batch 63, which contains 5.6% lanthana, the viscosity is much lower than in batches 64 and 1 at the same temperature, but the maximum rate of growth is about one-eighth of that observed in batch 1.

These observations suggest that the maximum rate of crystal growth can be affected by changing the viscosity of the system, or by adding larger cations (Ionic radii are listed in Table IV) which cannot be easily incorporated into the crystal which is growing in the glass. These large cations could become concentrated in the glass surrounding the growing crystal as the other cations (Mg^{++}, Al^{+++}, Si^{++++}) are being incorporated into the crystal. The factors limiting the maximum rate of crystal growth could be the diffusion of Mg^{++}, Al^{+++}, and Si^{++++} to the growing crystal and/or the diffusion of the foreign ions away from the crystal-glass interface. If this were the case, one would expect that the rate of change in size of the crystal as a function of time at a constant temperature would decrease as the concentration of foreign ions in the glass increased. Two representative growth curves for cordierite in batches 1 and 63 are shown in Fig. 5. It can be seen that, for these relatively short times, the rate of change of crystal length is linear as a function of time. It is probable that measurements with the electron microprobe could be useful in elucidating the mechanism by which the rate of crystal growth can be so significantly altered. These measurements could show concentration gradients within the glass which surrounds the crystal and also whether the yttria and the lanthana are incorporated into the cordierite crystal. It is well established that cordierite has channels extending through

FIG. 3

EFFECT OF TEMPERATURE UPON THE RATE OF GROWTH OF CORDIERITE IN BATCH 63

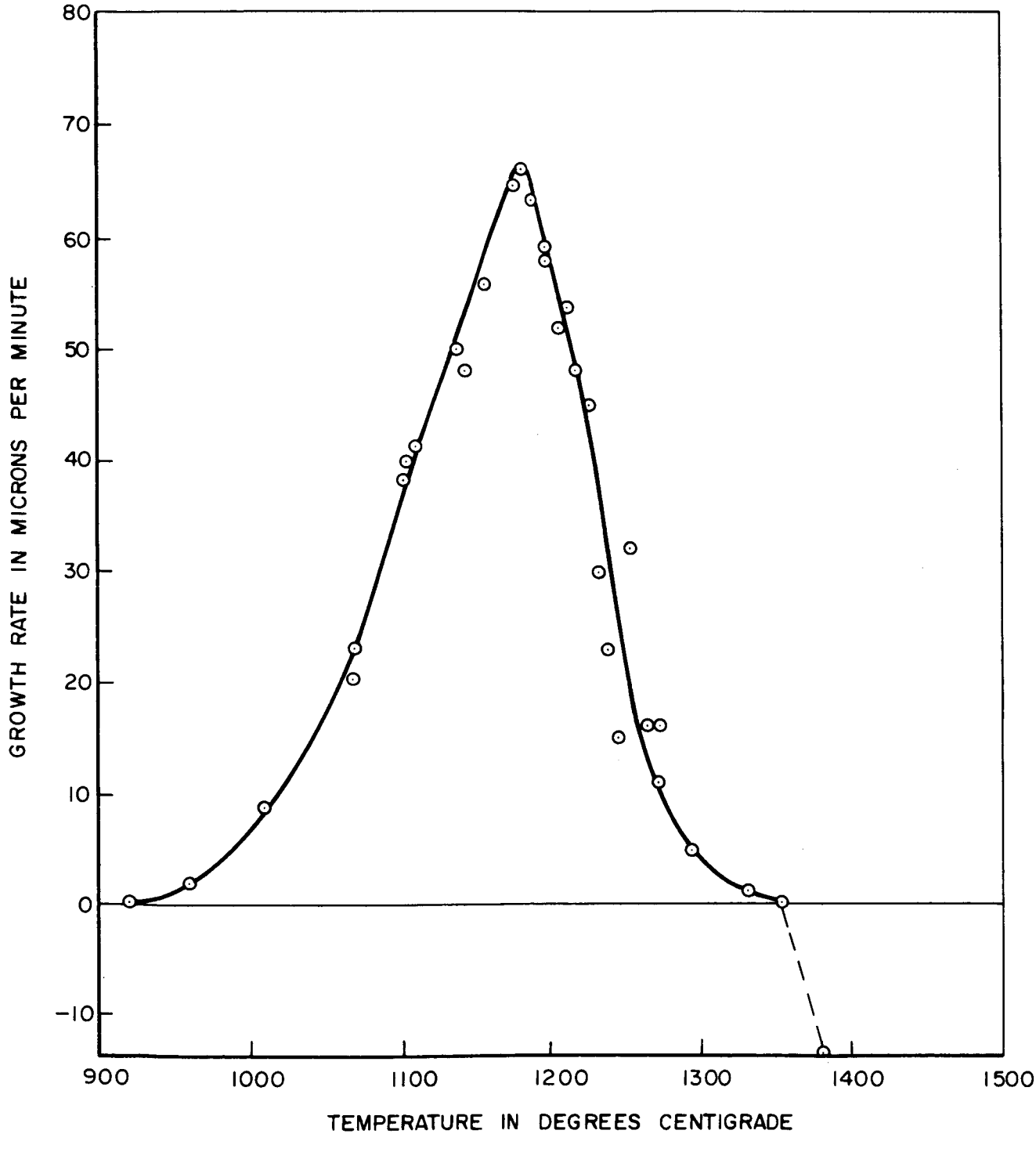

Table III

Rate of Growth of Cordierite in Batch 63

No.	Temp.	Rate	No.	Temp.	Rate
1	1189 ± 2	63	14	959 ± 4	2
2	1182 ± 2	66	15	1069 ± 2	23
3	900 ± 5	0 in. 10 min	16	1010 ± 3	9
4	1213 ± 2	54	17	1272 ± 2	11
5	1198 ± 2	59	18	1383 ± 2	-15
6	1156 ± 3	56	19	1353 ± 4	0 in. 30 min
7	1138 ± 2	50	20	1294 ± 2	5
8	1178 ± 3	65	21	1331 ± 4	1
9	1103 ± 2	40	22	1266 ± 2	16
10	1067 ± 4	20	23	1226 ± 2	45
11	1219 ± 3	48	24	1253 ± 2	32
12	1144 ± 4	48	25	1347 ± 2	slow solution
13	1272 ± 2	16	26	836 ± 2	0 in. 120 min

Table IV

Batch No.	Comp. (wt%)	Liquidus Temperature	Max. Growth Rate, μ/min	Temp. of Max. Growth Rate
1	51.1 SiO_2 29.7 Al_2O_3 18.9 MgO	1410 ± 3°	485	1225°
1-B	55.0 SiO_2 30.0 Al_2O_3 15.0 MgO	1435 ± 5°	300	1225°
64	51.66 SiO_2 27.92 Al_2O_3 17.20 MgO 3.12 Y_2O_3	1394 ± 2	190	1225
63	53.50 SiO_2 23.08 Al_2O_3 17.24 MgO 5.64 La_2O_3	1350 ± 5	66	1180

Ionic Radii in Angstroms*

Al^{+++} = 0.51
Mg^{++} = 0.66
Si^{++++} = 0.42
Y^{+++} = 0.92
La^{+++} = 1.14

*Ahrens, L. H., Geochim et Cosmochim. Acta, 2, (1952) p. 155-169

FIG. 4

VISCOSITY-TEMPERATURE CURVES FOR THREE GLASSES

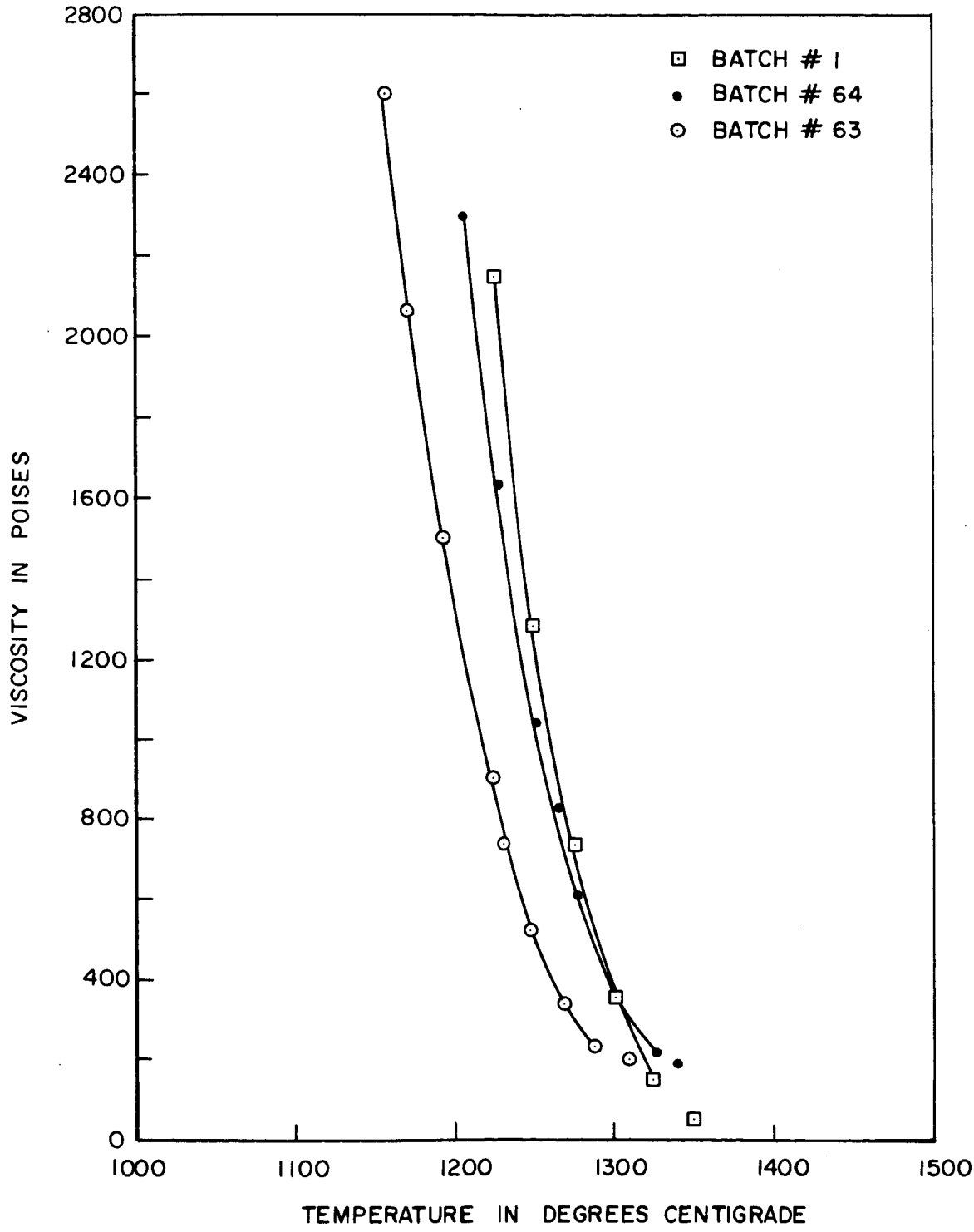

FIG. 5

REPRESENTATIVE GROWTH CURVES FOR CORDIERITE, THE INCREASE OF CRYSTAL LENGTH WITH TIME

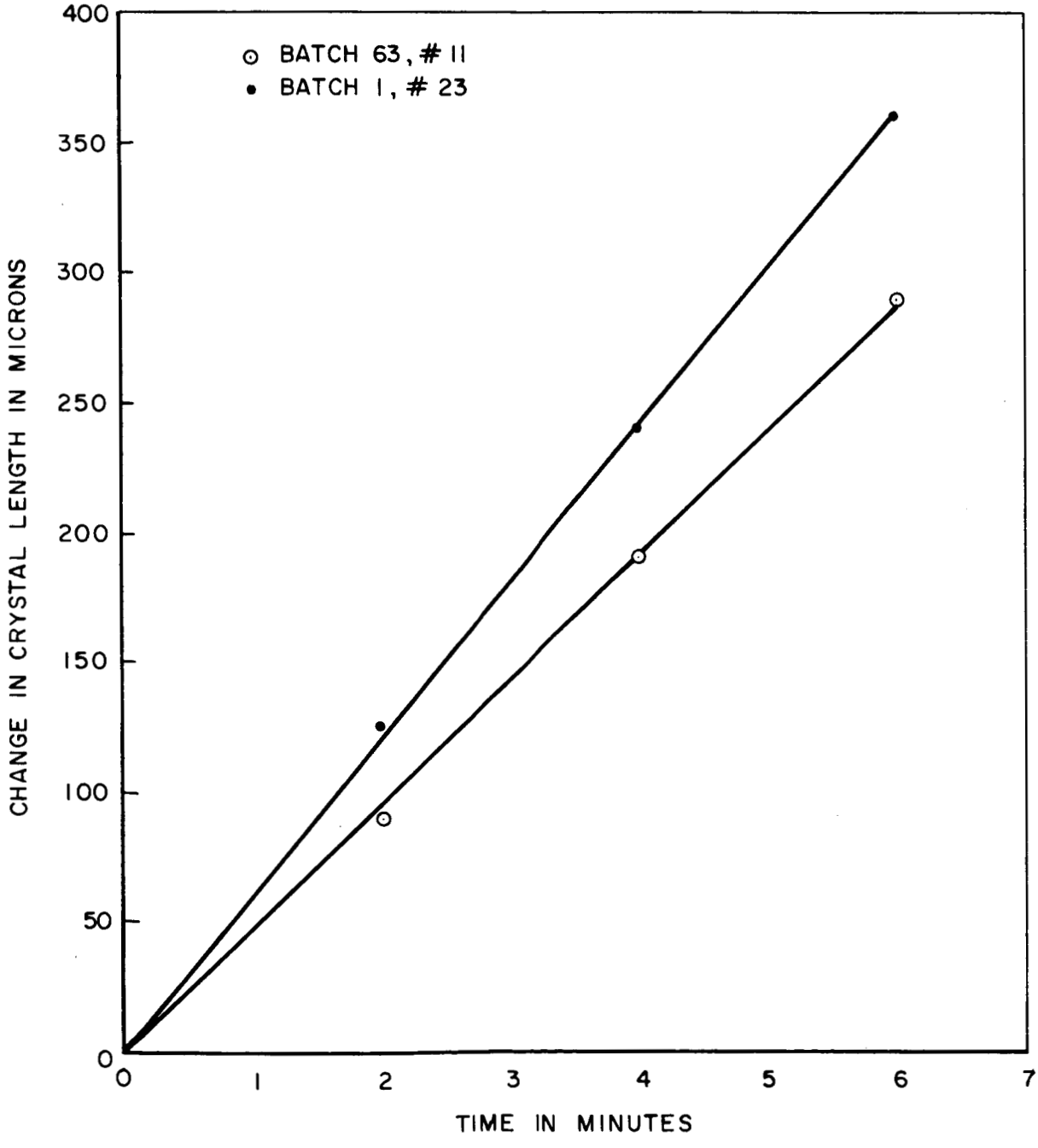

the crystal structure which are parallel to the "c" axis, which also is the direction of fastest growth. These channels which can contain alkali ions and water molecules should also be able to contain the yttrium and lanthanum ions. It may be possible that if these ions are incorporated into the crystal, they may cause a perturbation in a growth step, such as in a screw dislocation mechanism. Microprobe measurements could ascertain if these larger cations are contained in the crystal.

THE PRELIMINARY RESEARCH TOWARD THE ASSIGNMENT OF A MEANINGFUL VALUE TO THE STRENGTH OF GLASS FIBERS

Tensile Testing of Glass Fibers

Because of the sensitivity of glass fiber to surface damage that can be inflicted by winding on a drum, or other contact, and by exposure to uncontrolled atmosphere for a finite length of time, it has beome the practice to report so called "virgin strength" of freshly drawn glass fiber. This is accomplished by capturing a sample of fiber between the bushing and the winding drum, and measuring the tensile strength as soon as possible and before any obvious damage has occurred to the fiber. The difference in strength measured on glass fibers shortly after capture between bushing and winding drum, and measurements on fibers off the winding drum has been shown dramatically by W. F. Thomas (Ref. 1). Figure 6 compares the strength measured by Anderegg (Ref. 2) off the winding drum with Thomas' data for virgin fibers. Thomas considers that the dependence of strength on fiber diameter shown by the data of Anderegg and many other authors is the result of the greater susceptibility of the larger fibers to damage, and that the strength of glass fiber is independent of diameter provided that care is taken to avoid damage during sampling and testing. Of particular interest in the work of Thomas is the extremely low scatter in the strength data which he obtained on virgin fibers tested within ten minutes of capture. Typically, he found that in testing 50 samples of E glass fiber produced under the same experimental conditions, all samples had strengths between 530,000 and 560,000 psi.

Preliminary Experiments

Before attempting to measure the virgin strength of UAC experimental glasses, it was considered necessary to make measurements on a known glass using testing equipment and fiber producing facilities available in these laboratories for comparison with previously published results. E glass was selected for preliminary experiments since marbles of this composition could be obtained commercially, and because E glass has been extensively studied.

FIG. 6

STRENGTH OF GLASS FIBER

A - FIBERS OFF WINDING DRUM - DATA OF ANDEREGG (2)

B - VIRGIN FIBERS - DATA OF THOMAS (1)

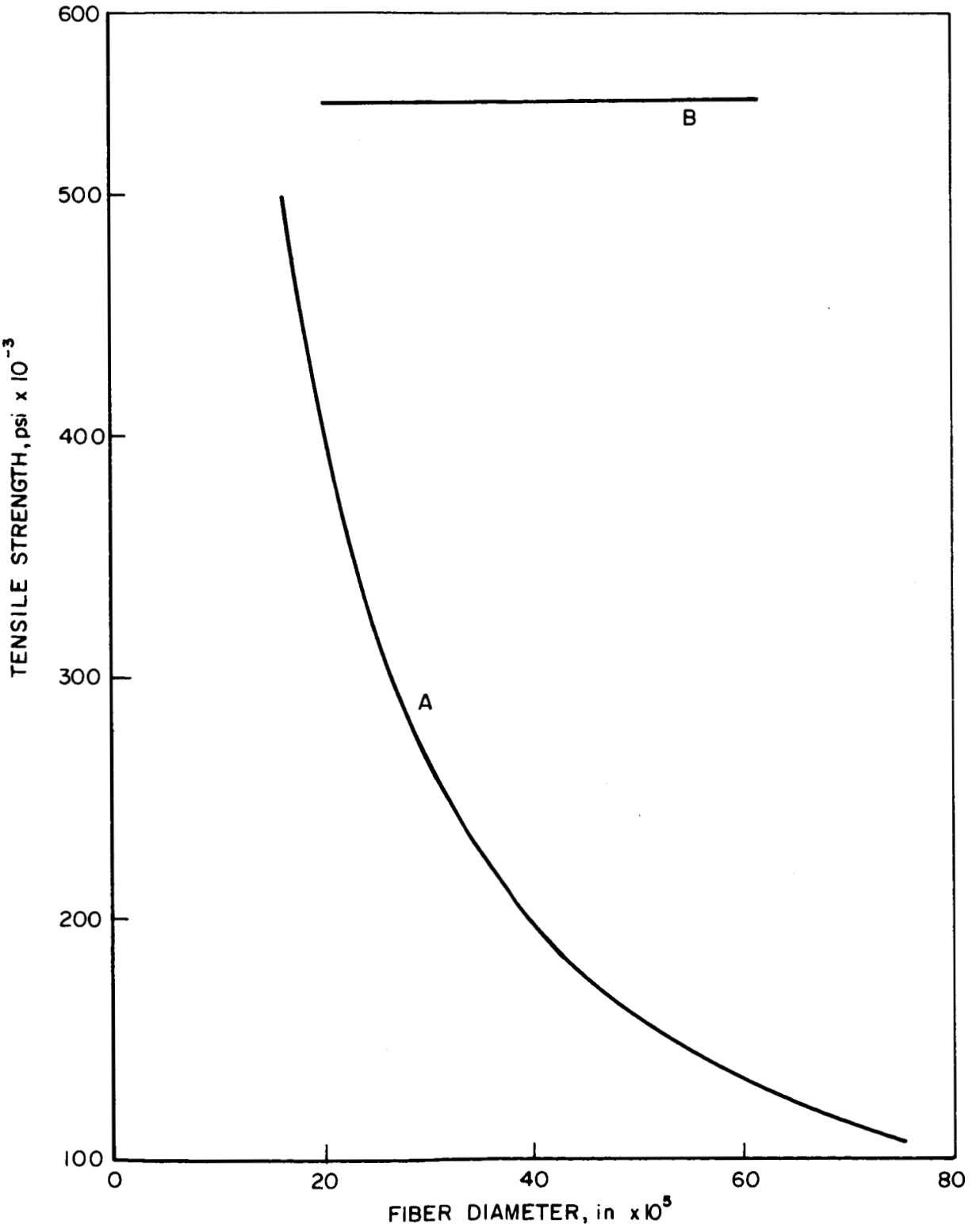

Fiberization Techniques

The fiberization equipment and technique previously described in Quarterly Progress Report No. 7 were used to produce E glass fibers varying in diameter from approximately 0.5 to 1.9 mils. In the first fiberization runs, E glass marbles were crushed to frit which was changed into the platinum crucibles. However, this procedure resulted in very seedy glass because of the many bubbles trapped in the molten glass. In subsequent runs, the as-received marbles were cleaned in an ultrasonic degreaser, rinsed several times with tap water, given a light etch with hydrofluoric acid, then rinsed and stored under distilled water until charged into the crucible. The reduction in seediness resulting from the latter procedure is shown in Fig. 7.

Fiber Capture

The capture device is shown in Fig. 8. This consists of two pairs of sheers actuated by a common lever. The inner sheer of each pair is made of 1/4 in. stock and the face addressing the fiber is coated with double-sided sticky tape. Attached to the outer sheer of each pair is a block which presses the fiber onto the tape an instant after the fiber has been sheared. With the sheers in the vertical position, the lower pair of sheers is adjusted so that it cuts the fiber an instant before the upper sheer closes so that the captured fiber is not in tension. After the fiber drawing process has been initiated and brought to a steady state at the desired experimental conditions, a sample is captured manually with the sheers.

Fiber Testing

The fiber testing machine used in these preliminary experiments, shown as Fig. 9, was developed at UAC, and has been described in the literature (Ref. 3). The fiber is mounted between the moving crosshead (A) and the stationary crosshead with red sealing wax which is melted by nichrome heaters underneath the fiber mounting tabs. The crosshead moves at a constant rate of 0.77 mm/min. The load cell which is mounted on the stationary crosshead is of the strain guage type, is temperature compensated, and responds only to load components in the direction of the fiber axis. An electronic bridge circuit monitors the load cell, which is calibrated by placing the test device in the vertical position and suspending laboratory weights from the load cell. The calibration curve for the load cell used in these experiments is shown in Fig. 10. The short term drift of the bridge circuit amounts to two percent of full scale deflection.

Immediately following fiber capture the fiber, still held by the sheers, is placed in position on the mounting tabs which have been preheated to melt the wax. The fiber was then cut free from the capture sheers and the wax allowed to harden. Without forced cooling of the tabs, the wax would become sufficiently hard to permit testing in about fifteen minutes. Subsequently, a pair of water

F910373-9

FIG. 7

E - GLASS TEAR DROPS

A FROM FRIT

B FROM MARBLES

FIG. 8

FIBER CAPTURE SHEARS

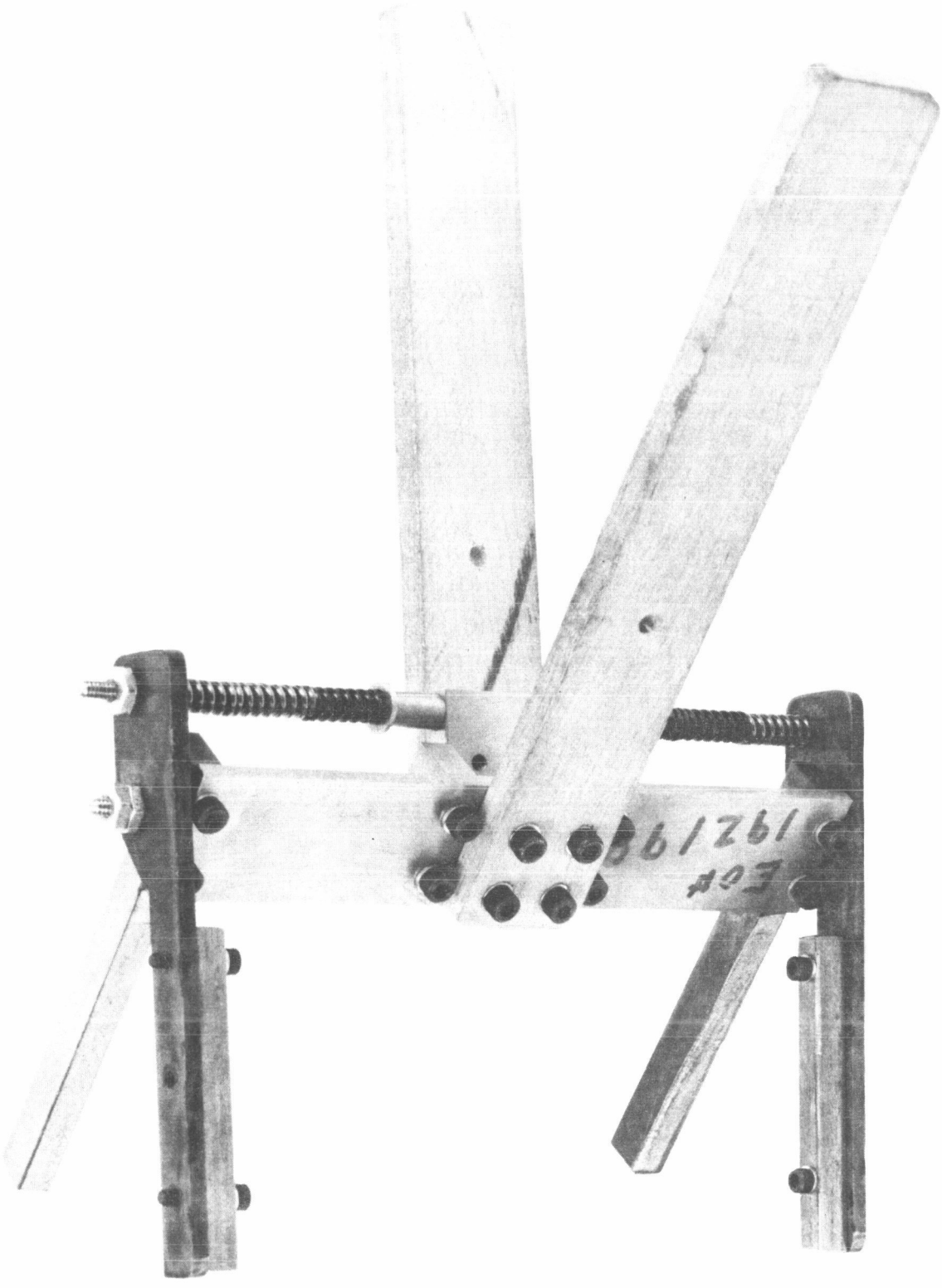

FIG. 9

TENSILE TESTER

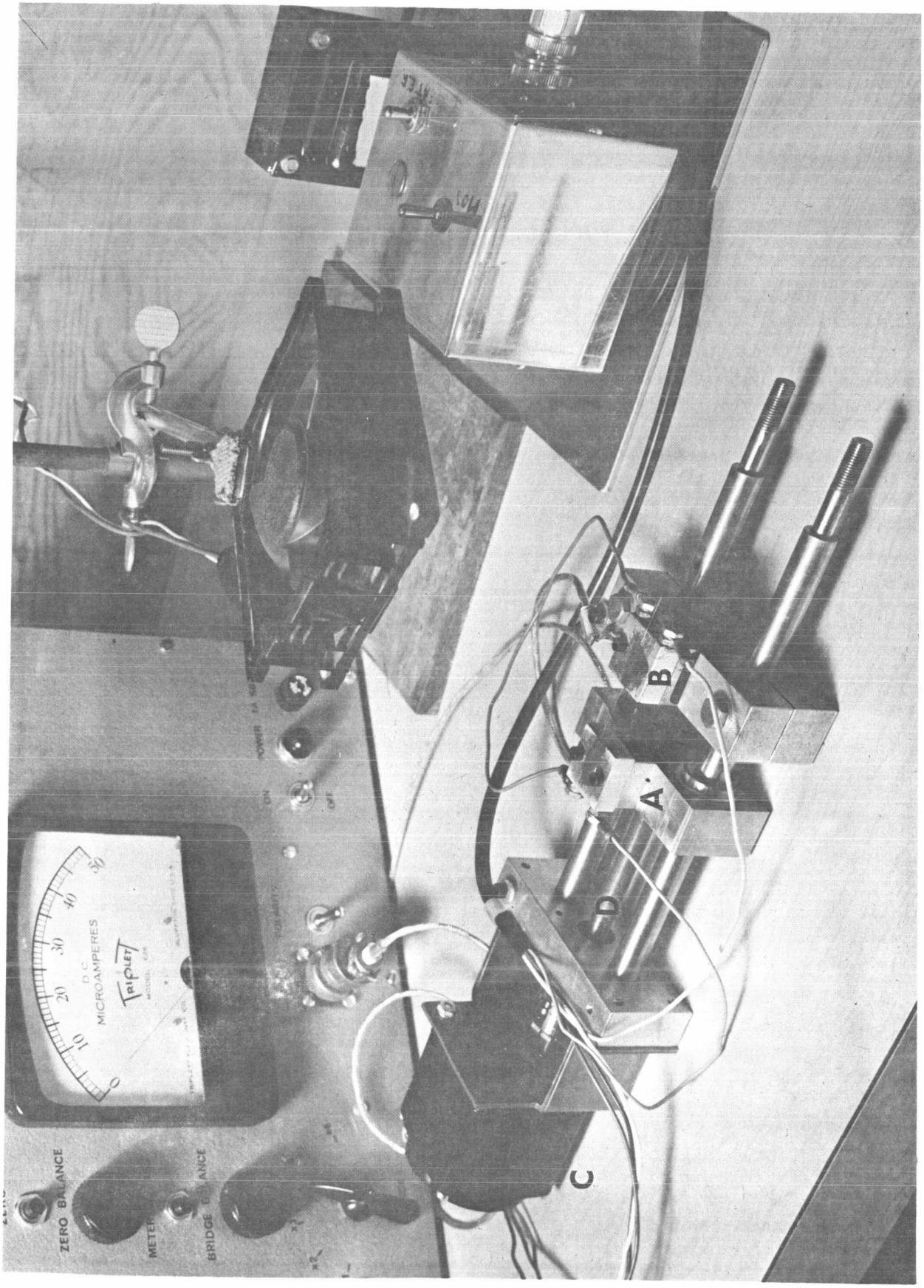

FIG. 10

CALIBRATION CURVE FOR TENSILE TEST APPARATUS

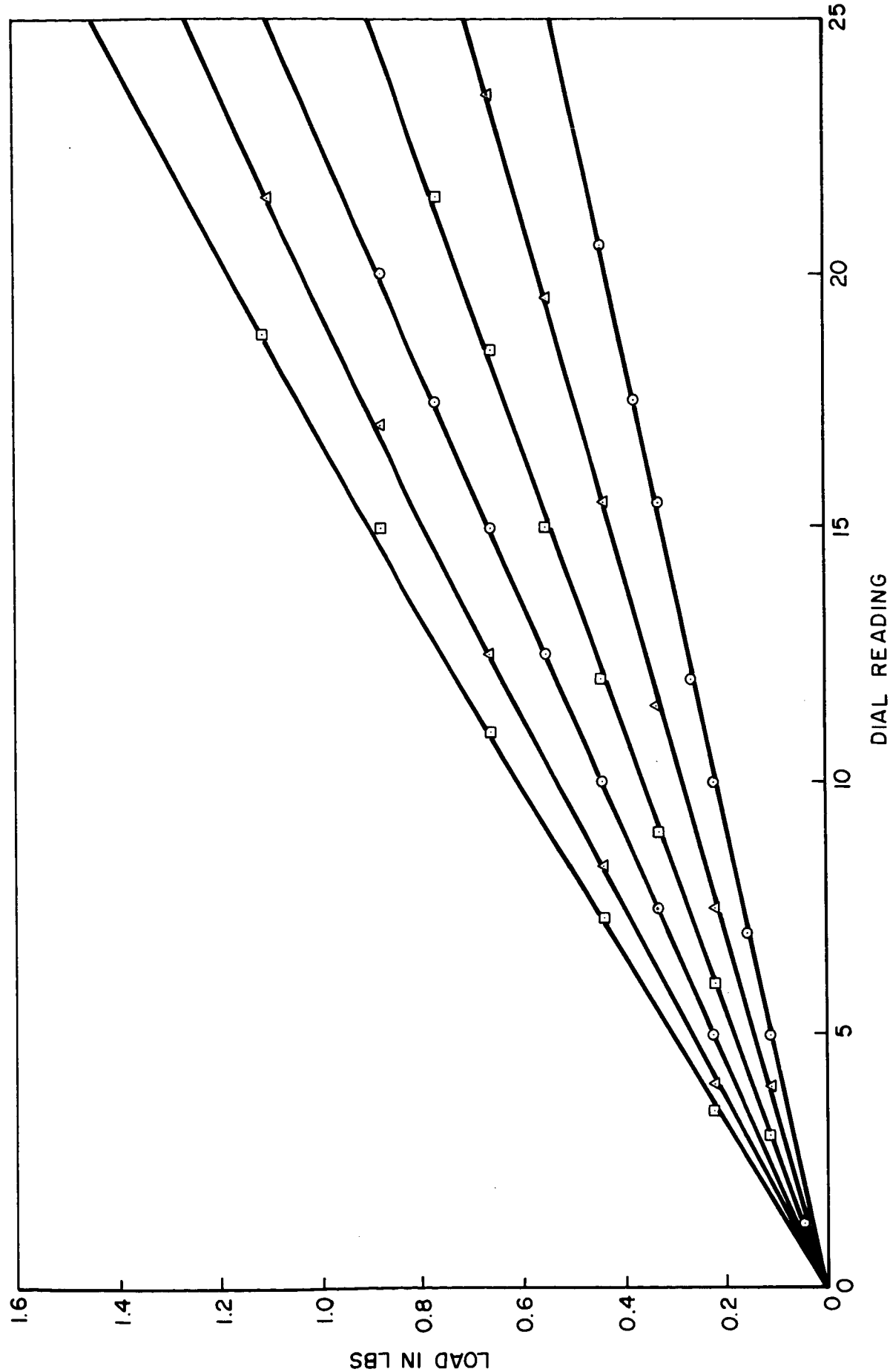

cooled tabs was affixed which permitted more rapid testing. A satisfactory cooling rate permitted testing about four minutes after capture. However, glass fibers mounted in the sealing wax slowly cooled or forced cooled frequently slipped, resulting in a jerky loading rather than a smooth loading rate.

As well as testing fibers captured as described above, spooled fiber was also tested after 5 days of normal laboratory storage to assess the effects of spooling and storage on fiber strength.

Two kinds of fracture were noted which we shall call "normal" and "fly-out". Low strength fibers (strength below about 300,000 psi), usually those that were measured after storage, exhibited "normal" fracture. In this case failure occurred within the guage length (approximately one inch) and the fiber ends on either side of the fracture were retained in the testing apparatus. In the case of fibers exhibiting strengths above 300,000 psi, after fracture, it was frequently found that the fiber was broken away at either grip, or sometimes broken away at one grip while still projecting from the other. Occasionally the fiber ends would be found projecting from both grips but the center section was missing. Attempts were made to photograph this mode of fracture. The fracture event could not be recorded at 500 frames per second; one frame of a film strip would show the intact fiber mounted in the testing machine, and in the next frame the fiber would be gone.

Measurement of Fiber Diameter

Several techniques for measuring fiber diameter were investigated and the results compared. These were: (1) mechanical measurement using a Johansen dial guage, (2) scaling of high magnification photographs of the fibers, and (3) use of a Watson two color split image eye piece in conjunction with the petrographic microscope. Measurement of lengths of fiber by all three methods gave the same fiber diameter to within one half of one percent. The Watson split image eye piece was adopted as the standard diameter measuring technique because of its greater convenience. The typical variation in diameter over a two inch length of glass fiber produced in the fiberizing equipment was five percent on fibers of nominally one mil diameter.

After breaking a sample in the testing apparatus, the fiber diameter was measured adjacent to the fracture where possible. In the case of "fly-out", diameter was measured on the section of fiber that extended beyond the outside of the mounting tabs.

Experimental Results

Strength data obtained for captured and spooled E glass fibers are recorded in Table V. The precision of the strength measurements S can be assessed by considering the uncertainty in the load measurement ΔL, and in the diameter measurement Δd from the equation

$$\frac{\Delta S}{S} = \frac{\Delta L}{\Delta} + 2\,\frac{\Delta d}{d} \qquad (1)$$

Table V

Strength Data

Sample Number	Pulling Temperature °C	Pulling Speed ft/sec	Elapsed Time from Capture to Testing (min)	Load at Failure (lbs)	Fiber Diameter (mils) ± 5%	Tensile Strength psi x 10^{-3}	Mode of Fracture	Notes
E-1	1237		~15	0.08 ± 0.01	1.02	90 ± 20	normal	
E-2								fiber damaged, not tested
E-3	1242	4.5	~15	0.34 ± 0.01	1.06	390 ± 50	fly out	
E-4	1244		~15	0.33 ± 0.01	1.13	330 ± 43	fly out	
E-5	1246		~15	0.26 ± 0.01	0.99	340 ± 47	fly out	samples E-1 through E-10, virgin strength
E-6	1248	6.2	~15	0.07 ± 0.01	0.85	120 ± 27	normal	measurements on glass fibers from seedy batch
E-7	1250	8.3	~15	0.22 ± 0.01	0.78	460 ± 67	fly out	see Fig. 7
E-8	1252	10.5	~15	0.07 ± 0.01	0.62	230 ± 55	normal	
E-9	1267	8.8	~15	0.11 ± 0.01	0.57	440 ± 83	fly out	
E-10								fiber damaged, not tested
E-11				0.11 ± 0.01	1.11	114 ± 22	normal	
E-12				0.27 ± 0.01	1.97	89 ± 11	normal	
E-13				0.41 ± 0.01	1.28	318 ± 40	fly out	samples E-11 through E-21 tested after storage on winding
E-14				0.10 ± 0.01	1.05	115 ± 30	normal	drum for five days
E-15				0.18 ± 0.01	1.06	204 ± 32	normal	
E-16				0.15 ± 0.01	1.11	155 ± 26	normal	
E-17				0.06 ± 0.01	0.605	208 ± 55	fly out	
E-18				0.52 ± 0.01	1.41	333 ± 40	fly out	
E-19				0.10 ± 0.01	1.05	116 ± 32	normal	
E-20				0.27 ± 0.01	1.37	184 ± 25	fly out	
E-21				0.12 ± 0.01	1.28	93 ± 17	normal	
E-22	1247	4.5	~15	0.465 ± 0.01	1.32	337 ± 41	fly out	samples E-22 through E-43 are virgin measurements on
E-23	1245	4.5	~15	0.465 ± 0.01	1.21	405 ± 49	fly out	relatively seed-free glass
E-24	1252	4.5	~15	0.77 ± 0.02	1.68	348 ± 44	fly out	
E-25	1264	4.5	~15	0.515 ± 0.02	1.52	285 ± 40	fly out	
E-26	1268	4.5	~4	0.88 ± 0.025	1.45	532 ± 68	fly out	
E-27	1268	4.5	~4	0.66 ± 0.025	1.61	336 ± 46	fly out	
E-28	1266	4.5	~4	0.64 ± 0.025	1.36	441 ± 61	fly out	
E-29	1262	4.5	~4	0.75 ± 0.025	1.45	454 ± 60	fly out	
E-30	1266	4.5	~4	0.75 ± 0.025	1.76	308 ± 41	fly out	
E-31	1267	4.5	~4	0.86 ± 0.025	1.56	448 ± 60	fly out	
E-32	1267	4.5	~4	0.77 ± 0.025	1.42	484 ± 64	fly out	
E-33	1255	4.5		0.66 ± 0.025	1.38	442 ± 61	fly out	
E-34	1264	4.5		0.73 ± 0.025	1.42	460 ± 62	fly out	
E-35	1281	4.5	~15	0.73 ± 0.025	1.39	480 ± 64	fly out	
E-36	1280	4.5	~15	0.64 ± 0.025	1.52	353 ± 49	fly out	
E-37	1270	4.5	~15	0.60 ± 0.025	1.49	343 ± 47	fly out	
E-38	1266	4.5	~15	0.73 ± 0.025	1.33	525 ± 70	fly out	
E-39	1251	16.3	~4	0.12 ± 0.01	0.720	296 ± 54	fly out	
E-40	1250	16.3	~4	0.14 ± 0.01	0.635	452 ± 77	fly out	
E-41	1252	16.3	~4	0.12 ± 0.01	0.727	290 ± 53	fly out	
E-42	1252	16.3	~4	0.14 ± 0.01	0.645	430 ± 73	fly out	
E-43	1252	16.3	~4	0.15 ± 0.01	0.560	607 ± 110	fly out	

Since fly-out prevents measurement of diameter at point of fracture, the relative uncertainty in the diameter was five percent since this was found to be the variation in diameter over a two inch length. The relative uncertainty in the load at fracture vaires with the load because of the short term drift in the electronics (two percent of full scale). Thus, there is a greater uncertainty in the load for fibers that failed at low loads than for fibers which failed at high loads. The uncertainty calculated for each strength value from equation (1) is recorded in Table V.

Except for 3 measurements (E-1, E-6, and E-8) all virgin fibers exhibited fly-out fracture and had strengths above about 300,000 psi. The three low values were obtained on fibers pulled from the seedy melt and presumably resulted from entrained bubbles. The remaining virgin strength measurements are plotted as a function of fiber diameter, with drawing temperature and elapsed time before testing as parameters in Fig. 11. Fibers tested from the winding drum after five days are plotted in Fig. 12.

Discussion

The virgin strength values are apparently random with no clear correlation with fiber diameter, forming temperature, or time until testing. Although some of the strength values are as high as those reported by Thomas (Ref. 1), the mean value of 415,000 psi is twenty percent lower, and the scatter of the strength values is two orders of magnitude greater, than those of Thomas. Winding fiber on a drum and testing after five days resulted in a mean strength lower by a factor of two than the mean strength of the virgin fibers. Before proceeding to test UAC experimental glass fibers, we shall attempt to improve on our sampling and testing facilities and techniques, both to increase the precision of individual strength measurements and hopefully, to reduce the scatter.

Several factors are suspect as sources of low strength values, and these will be investigated.

The strength measurements were made in the laboratory which is also used for batching and melting. Because of the need for ventilation and exhaust systems there are fairly strong drafts in the area. Although great care is exerted to maintain cleanliness, considerable airborne dust from batch materials is inevitable. Airborne dust particles impinging on the fibers before fracture could result in initiation of surface flaws that would decrease strength.

The fly-out type of failure exhibited by relatively high strength specimens leads to uncertainty as to the validity of a measurement, firstly because it is not possible to assess whether the initial failure was within the guage length or rather occurred at the grip as a result of superimposed bending stresses resulting from misalignment, and secondly because the fiber diameter cannot be measured at the point of fracture. Presumably, a fiber could fracture initially in the guage length, and as the fracture progresses, a bending moment would be imposed that would impart a whiplash to the ends of the fiber. The whiplash may

FIG. 11

VIRGIN STRENGTH OF E-GLASS FIBERS

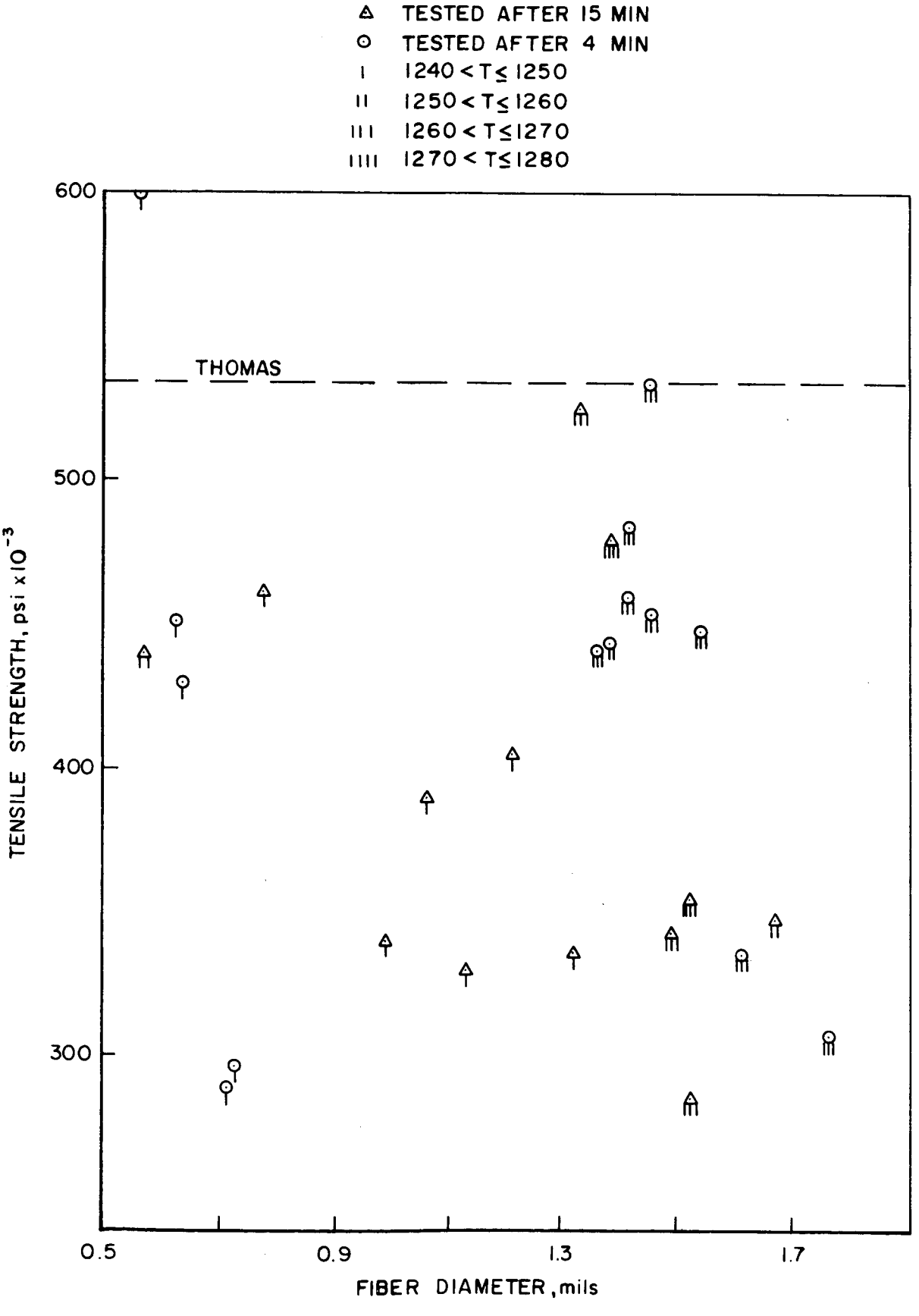

FIG. 12

STRENGTH OF E-GLASS FIBERS TAKEN OFF WINDING DRUM

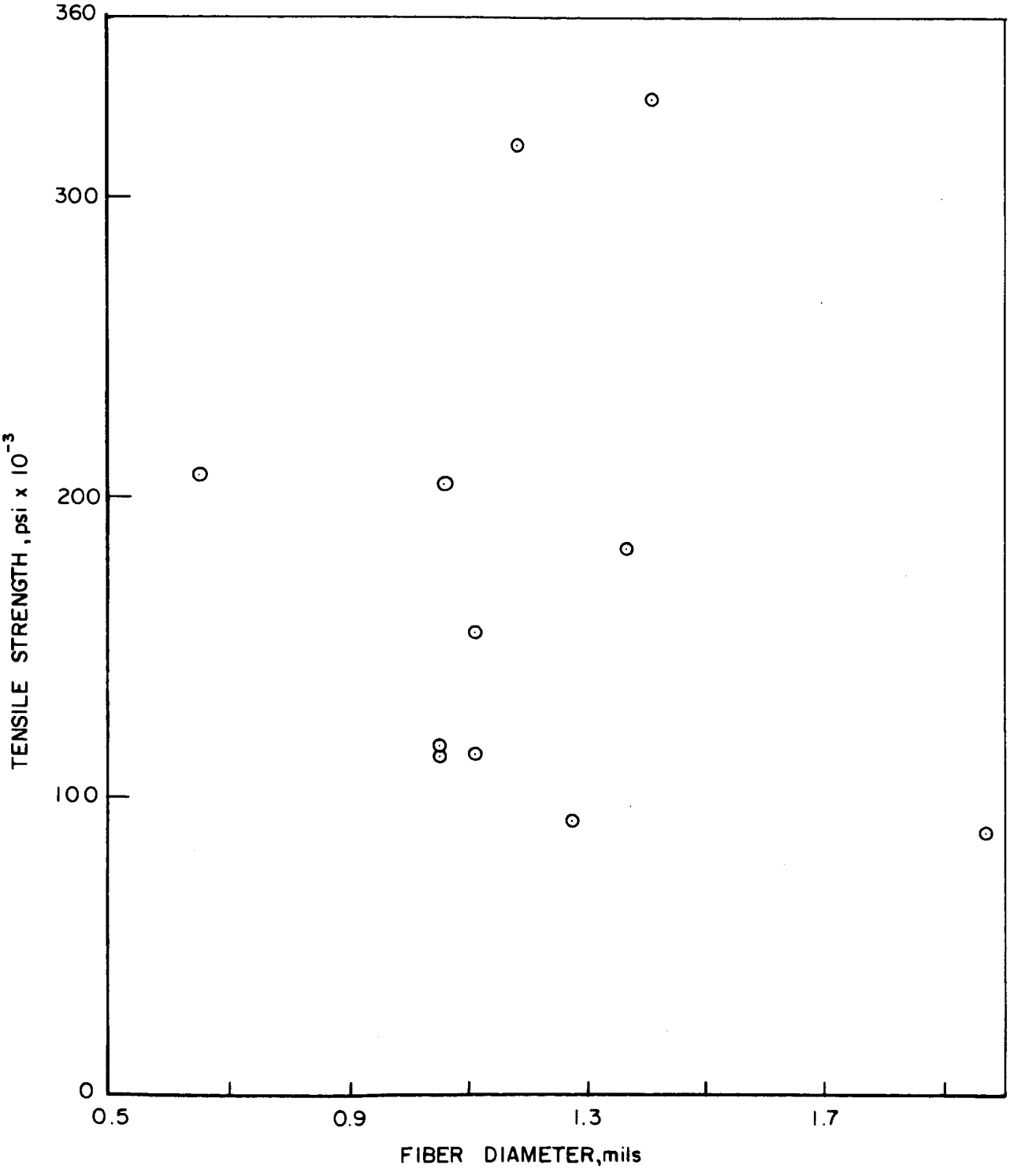

result in secondary fractures at or near the grips. Thomas (Ref. 1) does not report this fly-out mode of fracture. This may be because the damping dynamics of his test apparatus are substantially different from those of the test apparatus used in these experiments, and/or because the diameter of his fibers was smaller.

Another possible, and perhaps a major, source of low strength values also associated with the testing apparatus is slippage of the fiber in the grips. It has been observed that as the load is applied, although crosshead motion is uniform, the stress rate is not. The load will frequently fall momentarily during a test as the fiber slips in the wax, then rises again as the fiber is regripped. Thus, the fibers are subjected to stress transients of unknown magnitude rather than to the desired uniform strain rate.

Selection and Preparation of New Glass Systems for Evaluation

The thirty-seven new glass compositions devised, mixed and melted in this period included eight distinct groups of glass compositions as is readily apparent from Tables VIA, B, C, D. Possibly, the most unusual of these groups is that given in Table VIB based on Morey's optical glass patent (Ref. 4) with progressive substitution of yttria for lanthana and zirconia for tantalum oxide. These batches, in general, gave glasses of optical quality from which fibers could be pulled by hand with ease but from which we were completely unable to mechanically draw fibers using the simple UARL procedure described in our earlier reports.

The next most unusual glass batches are probably the two barium silicates listed in Table VIC. The purpose in working with these two very simple binary glass compositions is to attempt to produce glass fibers with two stable immiscible completely interpenetrating phases (Ref. 5) to see how such structures affect elastic modulus and strength. No attempt has been made to fiberize the glasses obtained from these batches as yet, since the high temperatures required can only be achieved in our platform kiln when all of the super-kanthal hairpins used in this kiln are relatively new.

The other twenty-nine compositions listed in the various parts of Table VI are closer to the types of glass batches melted earlier in this program. Compositions 182 through 187 contain more of the usual glass making ingredients than is customary in this research in an effort to tailor-make the characteristics of the glass batch to increase working range, decrease surface tension, decrease viscosity, and lower preparation temperatures. The group of compositions from 188 through 193 continue the usually high magnesia to alumina ratio selected on the basis of a previous UARL glass having high modulus to density ratio. Batches 203 through 205 are noteworthy inasmuch as they produce optical grade glasses without any alumina. Glasses 216 through 218 continue the study of calcium-aluminate glasses with only token amounts of silica.

TABLE VIA

New Experimental Glass Batches - Grams

Actual Ingredient	182	183	184	185	186	187
Silica	148.0	145.8	128.0	130.0	128.7	125.9
Alumina	---	30.9	---	27.6	---	26.7
Magnesia	47.2	40.3	42.1	36.0	41.3	34.8
Calcium Carbonate	86.2	54.6	77.2	48.8	81.1	65.4
Yttrium Oxalate	372.0	367.0	---	---	---	---
Cerium Oxalate	43.5	42.8	38.8	38.7	37.9	37.1
Samarium Oxalate	---	---	---	---	401.0	391.0
Lanthanum Oxalate	---	---	389.0	382.0	---	---
Vanadium Pentoxide	56.0	55.2	50.0	49.2	48.9	47.6
Zirconium Carbonate	8.45	8.39	7.55	7.37	---	---
Titania	24.6	24.3	21.9	21.6	21.5	21.0
Lithium Carbonate	22.7	22.3	20.3	20.0	19.8	19.25
Raw Earth Oxalate	---	---	---	---	---	---

	188	189	190	191	192	193
Silica	193.5	174.3	170.7	174.4	174.3	173.0
Alumina	40.4	36.5	35.9	36.6	36.5	36.8
Magnesia	79.7	72.1	70.7	72.2	72.2	67.0
Calcium Carbonate	---	---	---	---	---	---
Yttrium Oxalate	313.0	---	---	---	---	175.8
Cerium Oxalate	---	332.0	---	---	---	
Samarium Oxalate	---	---	343.0	---	---	---
Lanthanum Oxalate	---	---	---	330.0	---	204.7
Vanadium Pentoxide	70.75	64.0	62.8	64.0	64.0	63.5
Zirconium Carbonate	---	---	---	---	---	---
Titania	---	---	---	---	---	---
Lithium Carbonate	---	---	---	---	---	---
Raw Earth Oxalate	---	---	---	---	331.0	---

TABLE VIB

New Experimental Glass Batches - Grams

Actual Ingredient	194	195	196	197	198	199
Lanthanum Oxalate	222.5	268.5	---	---	---	---
Thoria	40.0	54.4	59.8	67.0	60.0	76.8
Barium Carbonate	57.5	75.5	82.0	92.8	77.2	89.7
Fused B_2O_3	110.0	143.8	156.3	177.0	150.0	174.0
Tantalum Pentoxide	65.0	76.2	82.7	---	90.0	---
Vanadium Pentoxide	---	43.9	47.7	54.0	---	---
Yttrium Oxalate	---	---	248.5	282.0	374.0	414.0
Zirconium Carbonate	---	---	---	28.65	---	28.8

TABLE VIC

New Experimental Glass Batches - Grams

Actual Ingredient	200	201	202	203	204	205
Silica	165.5	165.7	154.7	212.6	201.3	176.4
Alumina	78.2	78.1	73.0	---	---	---
Magnesia	66.1	66.0	61.7	101.2	97.6	83.7
Yttrium Oxalate	208.0	207.5	---	499.0	478.0	---
Lanthanum Oxalate	243.0	---	226.0	---	---	478.0
Cerium Oxalate	---	241.5	227.5	---	46.8	52.9
Calcium Carbonate	---	---	---	---	---	---
Barium Carbonate	---	---	---	---	---	---

Actual Ingredient	206	207	208	209	210	211
Silica	185.0	164.1	193.0	172.5	154.8	381.0
Alumina	83.9	80.8	87.8	81.9	73.2	---
Magnesia	---	68.3	74.1	69.2	61.8	---
Yttrium Oxalate	372.0	502.0	382.0	367.0	---	---
Lanthanum Oxalate	---	---	---	---	378.0	---
Cerium Oxalate	---	---	---	84.8	75.9	
Calcium Carbonate	164.2	---	---	---	---	---
Barium Carbonate	---	---	---	---	---	154.0

Actual Ingredient	212
Silica	321.0
Alumina	---
Magnesia	---
Yttrium Oxalate	---
Lanthanum Oxalate	---
Cerium Oxalate	---
Calcium Carbonate	---
Barium Carbonate	257.0

TABLE VID

New Experimental Glass Batches - Grams

Actual Ingredient	213	214	215	216	217	218
Silica	197.0	323.0	224.0	33.0	---	63.3
Alumina	13.6	55.0	---	173.0	178.5	156.3
Magnesia	---	123.0	22.6	---	---	---
Calcium Carbonate	---	---	287.0	515.0	528.0	458.0
Barium Carbonate	---	---	35.3	---	32.2	31.8
Lanthanum Oxalate	627.0	---	---	---	---	---
Cerium Oxalate	---	---	---	---	---	---
Yttrium Oxalate	---	---	---	---	---	---
Titania (not Rutile)	---	---	73.0	---	---	---
Zirconium Carbonate	---	---	46.6	---	---	---

All of these experimental glasses are prepared in the usual 500 gram batch using high purity (99.9%) alumina crucibles in air in the UARL super-kanthal hairpin kilns. The ingredients in general are completely mixed dry by tumbling and pelletized to facilitate handling. No fining agents are added to the batches since the use of at least one constituent as either the oxalate or carbonate has proven sufficient in general to yield optical quality glass free of seed and bubbles when the mix is held at a temperature of 1540°C or higher for a period of two hours. The highly tinctorial materials used in some of the batches does, however, eliminate any possible optical examination of some of the glasses obtained but it is presumed that such materials did not result in inferior quality glass.

Characterization of Glass Fibers Mechanically Drawn from Experimental Glass Compositions

In Table VII is listed all the data obtained to date on the measurement of Young's modulus on fibers machine drawn from the experimental glass batches. These results are for the most part obtained on specimens measured for us by Lowell Institute of Technology using an Instron CRE tester operated with a machine speed of 0.2 in. per minute, a chart speed of 20 in. per minute, a gage length of 5 in., and a full scale capacity of 1.0 pounds. Air actuated clamps with flat rubber coated faces are used at Lowell for holding the test specimens.

Twenty specimens were taken from approximately the center portion of each spool. The specimens were eight inches long, with about one yard of fiber being discarded between each specimen. It was not always possible to select fibers in exactly this manner because many of the spools had discontinuous odd lengths of fiber, but in general, the specimens selected represent the middle 20 yards of fiber received for testing.

Three fiber diameter measurements were made in the middle three-inch portion of each eight-inch specimen. Measurements were made using a monocular microscope equipped with an eye piece reticule and operated with a magnification of 774 (18x eye piece, 42x objective). Each reticule division was equal to 0.092 mils.

The average of the twenty determinations for each fiber is shown in Table VII together with the maximum and minimum value of modulus obtained. As was shown in our last report, the standard deviation for twenty observations is typically 1.82 million psi, i.e. a value such as the 16.4 million psi measured for UARL glass 126 can be said with 99% probability to lie between 15.2 and 17.6 million psi. This has been again confirmed in this quarter since twenty repetitive runs on freshly prepared samples of UARL experimental glass 129 gave an average value of 16.9 million psi compared to the value of 16.5 million psi on twenty samples from the original melt of this glass.

From this point of view, therefore, it is possible that we have not attached sufficient significance to the extremely high maximum modulus value noted on three occasions. For example, UARL glass 166 yielded a maximum modulus measurement of 31.5 million psi, UARL glass 159 a maximum modulus measurement of 27.4 million psi, and UARL glass 40 a maximum modulus measurement of 29.2 million psi.

Recapitulation of All Data for Elastic Modu

Composition in Mol Percent

Glass Number	SiO_2	Al_2O_3	MgO	CaO	Y_2O_3	La_2O_3	Ce_2O_3	Sm_2O_3	Ta_2O_5	ZrO_2	BeO	Na_2O	Li_2O	P_2O_5	ZnO	TiO_2	Glass
14	52.3	18.7	29.2														14
25	49.5	20.4	11.1								17.8						25
40	58.4	20.9	16.3				4.53										40
56	67.8												26.8	0.37	4.91		56
62	54.6	15.2	29.2				1.0										62
63	54.6	15.6	28.9			0.95											63
64	54.6	15.5	28.8		1.39												64
64																	64
65	54.6	15.6	28.9					0.89									65
66	53.7	15.3	28.3							2.56							66
67	54.7	15.3	29.3						0.76								67
68	53.4	18.3	28.8														68
69	57.3	14.6	28.0														69
70	55.3	12.6	29.3		2.83												70
70																	70
71	49.4	14.1	36.5														71
72	56.9	15.1	25.4				2.60										72
73	59.1	8.66	26.4		3.13		2.70										73
74	56.1	9.6	30.0		4.3												74
75	61.2			21.2								17.6					75
76	61.9			26.2								11.9					76
77	61.2			31.8								7.0					77
82	54.3	24.5	18.1							1.6		0.05					82
83	42.9		11.3	11.8			0.86			0.81	22.2		5.06			5.06	83
97	65.0		7.0	7.0	7-K_2O, 7-SrO, 7-BaO												97
98	55.0		9.0	9.0	9-K_2O, 9-SrO, 9-BaO												98
102	45.0	11.0	11.0	11.0									11.0		11.0		102
108	65.0		7.0	7.0	7.0								7.0		7.0		108
110	55.56	22.22	22.22														110
114	51.7	22.5	15.8		10.0												114
126	49.67	22.5	13.83		14.0												126
127	60.0	10.0	20.0		10.0												127
129	50.0	13.33	26.67		10.0												129
131	70.0	6.66		13.3	10.0												131
135	54.3	15.6	28.9			1.0											135
136	53.3	15.6	28.9			2.0											136
137	51.3	15.6	28.9			4.0											137
138	47.3	15.6	28.9			8.0											138
140	47.3	15.6	27.9			8.0	1.0										140
155	49.4	7.05	36.5						7.05								155
157	49.4	7.1	36.5						7.1 V_2O_5								157
159	57.4	6.6	28.0		8.0												159
160	57.4	6.6	28.0			8.0											160
161	57.4	6.6	28.0					8.0 rare earth oxides									161
166	51.7	23.0	18.3					7.0 V_2O_5									166

82 - Houze Glass - U.S. 3,044,888
83 - Owens-Corning - U.S. 3,122,277 (BeO)

Table VII

uli of Glasses Successfully Made Into Mechanically Drawn Fibers

Number	Density gms/cm^3	Dynamic Moduli Values: Velocity C (cm/sec) x 10^5 (FAB)	Velocity C (cm/sec x 10^5) UARL-1	Velocity C (cm/sec x 10^5) UARL-2	Velocity C (cm/sec x 10^5) Morgan	Velocity C (cm/sec x 10^5) Most Probable	c^2-cm^2/sec^2 x 10^{10}	ρc^2 = E(kg x 10^5/cm^2)	E(dynamic) psi x 10^6	Static Moduli Values: E(static) min psi x 10^6	Lowell E(static) max psi x 10^6	Lowell E(static) aver psi x 10^6 20 tests	UARL Static E psi x 10^6	WPAFB Static E psi x 10^6	(10 tests) psi x 10^6 UARL(static) Bulk E
5	2.5672														15.07
2	2.9574	5.74	5.12			5.74	32.9	9.72	13.80	9.5	16.3	12.3			
6	2.4368	5.79	6.20		5.78	5.79	33.5	8.16	11.60	9.3	29.2	16.2			
2	2.7036	6.51	6.32		6.29	6.31	39.8	10.75	15.30	8.9	12.4	10.7			
5	2.6847	6.37	6.65	6.18	6.53	6.43	41.3	11.10	15.78	13.1	15.4	14.0	14.7		
2	2.6818	6.26	5.95		6.03	5.99	35.9	9.63	13.67	9.0	16.7	13.0	14.4	13.7	14.71
										10.9	24.3(18.9)	14.7			14.78
															15.57
5	2.7197	6.24	6.51			6.375	40.7	11.07	15.75	12.3	15.2	13.8			15.20
2	2.6112		6.63			6.63	43.9	11.69	16.63	12.0	19.4	14.6			15.14
2	2.6535	6.58	6.58			6.58	43.3	11.47	16.33	10.0	15.9	12.7			
3	2.6295	6.58	6.52		6.54	6.55	42.9	11.27	16.05	11.8	17.1(14.9)	13.7			15.36
2	2.5910	6.39	6.52			6.455	41.7	10.4	14.80	11.9	15.3	13.6			
2	2.7526	6.58	6.41	6.33	6.44	6.44	41.5	11.42	16.25	10.2	18.4	13.5	14.9	13.6	15.23
										11.0	16.6	13.3			
1	2.6627		6.85			6.85	46.9	12.48	17.75	9.5	16.6	13.7			
2	2.8877	6.06	6.09	6.25		6.08	37.0	10.69	15.20	8.4	17.7(15.4)	12.5			(15.14)15.15
3	3.0152	6.125			6.05	6.09	37.1	11.02	15.70	12.8	19.7	15.1	13.5		15.14
	2.9983		5.92			5.92	35.0	10.5	14.95	11.4	19.5(17.2)	13.8			
	2.6340		5.69			5.69	32.4	8.53	12.12	5.0	19.3(14.1)	9.8			
			5.64			5.64	31.8			8.2	14.8	10.4			11.51
			5.53	5.78		5.66	32.0			9.0	13.1	11.0			12.16
2	2.5875	6.49	6.65	6.57		6.61	43.7	11.30	16.08	11.2	15.9	13.3			
2	2.8376	6.527	6.4975			6.512	42.4	12.03	17.11	11.9	20.9	15.35			
	2.8426									7.5	14.6	10.4			
	2.9168									6.0	15.1	10.8			
2	2.9188		4.82			4.82	23.25	6.79	9.66	8.0	21.6(17.1)	13.3			
										6.8	17.2	12.5			
	2.6128									9.9	18.5	13.8			
3	3.2237	6.12	6.396	5.93	6.68	6.28	39.4	12.72	18.10	8.3(12.3)	19.0	15.1	17.4	14-17	16.5
3	3.4634	6.00				6.00	36.0	12.44	17.72	11.4	19.7	16.15			
3	3.2553	6.06	6.09			6.075	36.9	12.62	17.12	12.7	19.4	15.2			
3	3.3105	6.03	6.36			6.195	38.4	12.70	18.08	11.0	21.8	16.7			
3	3.1200	5.89	5.86			5.87	34.4	10.73	15.28	10.0	16.6	12.5			
2	2.6303	6.16				6.16	37.9	9.98	14.19	11.4	16.7	13.3			
2	2.8035	6.08				6.08	37.0	10.37	14.75	10.6	17.9(15.9)	13.5			
3	3.0834	6.08				6.08	37.0	11.4	16.22	11.1	17.6	13.9			
3	3.5498	5.66				5.66	32.0	11.36	16.15	6.2	16.0	12.2			16.53
			5.64			5.64	31.8			13.4	17.2	15.0			
	3.2541									9.6	17.3	14.7			
	2.6962									8.5	18.6	13.1			
	3.2216									11.5	20.7	15.7			
	3.2211									8.9	21.3	14.6			
	3.4523									11.7	16.6	14.3			
	2.6930									7.5	31.5	13.6			

The statistics make it appear likely that these values are not mere flukes. This becomes particularly true since all three of these glasses belong to the same specialized glass family. Can there possibly be a microstructure present in some samples of these glasses which can account for these startlingly high values of Young's modulus? We are launching an intensive two pathed investigation to see if there are any truths in these observations by both looking with transmission electron microscopy for structure in these glasses and by purposely melting glasses known to show structures such as two immiscible liquid phases (Refs. 5 through 27).

REFERENCES

1. Thomas, W. F., Phys. & Chem. Glass 1, 4-18 (1960).

2. Anderegg, F. O., Ind. & Eng. Chem. 31, 290-298 (1939).

3. Schile, R. D. and G. A. Rosica, Rev. Sci. Instruments 38, 1103-1104 (1967).

4. U. S. Patent 2,150,694, George W. Morey to Eastman Kodak Company, issued March 14, 1939.

5. Argyle, J. F. and F. A. Hummel, Phys. Chem. Glass 4, 103-105 (1963).

6. Averjanov, V. I., N. S. Andreyev and E. A. Porai-Koshits, In "Physics of Non-Crystalline Solids" (J. A. Prins, ed.), pp. 580-588, North-Holland Publishing Company, Amsterdam (1965).

7. Cahn, J. W. and R. J. Charles, Phys. Chem. Glass 6, 181-191 (1965).

8. Glasser, F. P., I. Warshaw and R. Roy, Phys. Chem. Glass 1, 39-45 (1960).

9. Hafner, H. C., N. J. Kreidl and R. A. Weidel, J. AM. Ceram. Soc. 41, 315-323 (1958).

10. Haller, W., J. Chem. Phys. 42, 686-693 (1965).

11. Hammel, J. J., VII International Congress on Glass, Brussels. Paper 36 (1965).

12. Herczog, A., J. Am. Ceram. Soc., 47, 107-115 (1964).

13. Hirayama, C., J. Am. Ceram. Soc. 44, 602-606 (1961).

14. Ohlberg, S. M. and J. J. Hammel, VII International Congress on Glass, Brussels. Paper 32 (1965).

15. Owen, A. E., Phys. Chem. Glass 2, 87-98, 152-162 (1961).

16. Owen, A. E., Phys. Chem. Glass 3, 134-138 (1962).

17. Rockett, J. J., W. R. Foster and R. G. Ferguson, J. Am. Ceram. Soc. 48, 329-331 (1965).

REFERENCES (Contd.)

18. Roy, R., In "Symposium on Nucleation and Crystallization in Glasses and Melts" (M. K. Reser, G. Smith and H. Insley, eds), pp. 39-46, American Ceramic Society, Columbus (1962).

19. Roy, R., J. Am. Ceram. Soc. 43, 670-671 (1960).

20. Schroder, J., Angew. Chem. Internat. Edit. 3, 376 (1964).

21. Skatulla, W., W. Vogel and H. Wessel, Silikattechnik, 9, 51-62 (1958).

22. Tran, T. L., Glass Technol. 6, 161-165 (1965).

23. Vogel, W., Silikattechnik 10, 241-250 (1959).

24. Vogel, W. and K. Gerth, Glastech. Ber. 31, 15-27 (1958a).

25. Vogel, W. and K. Gerth, Silikattechnik 9, 353-358 (1958b).

26. Vogel, W. and K. Gerth, In "Symposium on Nucleation and Crystallization in Glasses and Melts" (M. K. Reser, G. Smith and H. Insley, eds), pp. 11-22, American Ceramic Society, Columbus (1962).

27. Vogel, W. and H. G. Byhan, Silikattechnik 15, 212-8, 239-44, 324-8 (1964).